Article

Sediment Mercury, Geomorphology and Land Use in the Middle Araguaia River Floodplain (Savanna Biome, Brazil)

Lilian Moraes [1,*], José Vicente Elias Bernardi [2], João Pedro Rudrigues de Souza [3], Joelma Ferreira Portela [3], Ludgero Cardoso Galli Vieira [1], Carlos José Sousa Passos [1], Jurandir Rodrigues de Souza [3], Wanderley Rodrigues Bastos [4], Lucas Cabrera Monteiro [2], Ygor Oliveira Sarmento Rodrigues [2] and José Garrofe Dorea [5,†]

[1] Programa de Pós-Graduação em Ciências Ambientais, Faculdade UnB Planaltina, Universidade de Brasília, Planaltina 73345-010, DF, Brazil; ludgero@unb.br (L.C.G.V.); cjpassos@unb.br (C.J.S.P.)
[2] Laboratório de Geoestatística e Geodésia, Faculdade UnB Planaltina, Universidade de Brasília, Planaltina 73345-010, DF, Brazil; bernardi@unb.br (J.V.E.B.); ygorsarmento@gmail.com (Y.O.S.R.)
[3] Laboratório de Química Analítica e Ambiental, Instituto de Química, Universidade de Brasília, Brasília 70919-970, DF, Brazil; joaoprsouza@outlook.com (J.P.R.d.S.); portela.joelma@gmail.com (J.F.P.); rodsouza@unb.br (J.R.d.S.)
[4] Laboratório de Biogeoquímica Ambiental Wolfgang C. Pfeiffer, Universidade de Rondônia, Porto Velho 76815-800, RO, Brazil; bastoswr@unir.br
[5] Faculdade de Ciências da Saúde, Universidade de Brasília, Brasília 70910-900, DF, Brazil
* Correspondence: lilian.moraes@gmail.com; Tel.: +55-61-999310801
† In memoriam.

Abstract: In order to assess the influencing factors of the presence of mercury in a river within the Savanna biome (Cerrado), we surveyed total mercury (THg) in bottom sediment from 50 lakes along 750 km of the Middle Araguaia floodplain. The sampling sites included non-urban and urban surroundings over three distinct geomorphologies. We measured water physicochemical parameters at each site and tested statistically if land use nested within the geological formation influenced the THg concentration in bottom sediments and related water parameters. Multivariate results indicate that the interaction between geological groups and land use is statistically significant ($p < 0.05$). Nested ANOVA and Tukey HSD tests confirmed that the geological formation with its nested land use influences the THg, pH, DO, conductivity, and TDS ($p < 0.05$). THg was significantly lower in Quaternary terrains ($p < 0.05$) and differed significantly between non-urban and urban areas in Neoproterozoic terrains ($p = 0.02$). The spatial projections of the THg eigenvector on the main axes with the scoring factors of the Neoproterozoic/Paleoproterozoic terrains, and urban/non-urban, confirmed the spatial correlations. These results indicate that the association of land use and geology could be the main driver of THg in the bottom sediments of lakes from the Middle Araguaia floodplain.

Keywords: geology; urbanization; nested; Cerrado; Hg; aquatic environment

1. Introduction

Mercury (Hg) is one of the most toxic chemical elements and a global environmental pollutant naturally available in the lithosphere, although it is also released from anthropogenic sources [1]. Natural emission sources are represented by geogenic processes (primary emissions), such as rock weathering and volcanic eruptions [2]. Concerning rock weathering, mercury concentrations vary according to the constitution of the rock, influencing the amount of mercury mobilized into the environment [3]. Along these lines, a recent study in Australia indicated that the highest mercury concentrations in sediments were determined in lakes associated with intrusive mafic igneous rocks originating from volcanic formations [4]. Volcanic and mafic rocks contribute to mercury's binding capacity

in freshwater wetland sediments [5], and Hg-rich regions are associated with these rocks, in an order of magnitude greater than in most other crustal lithologies, including sedimentary rocks [6]. However, anthropogenic emissions have altered the distribution of mercury on a global scale, so the increase in atmospheric mercury concentrations has resulted in a 300% increase in natural deposition rates [7].

The main anthropogenic sources of mercury in the southern hemisphere are artisanal and small-scale gold mining (ASGM), deforestation, and forest fires [8]. In Brazil, rapid and large-scale deforestation is a cause for concern. Environmental monitoring data indicate that deforestation destroyed approximately 6,606,499 hectares between 2019 and 2022, with the most significant negative impact observed in the Amazon rainforest (58%) and Cerrado (Brazilian Savanna) (32%) biomes [9]. Deforestation directly influences the atmospheric emission of mercury contained in terrestrial ecosystems and the transportation of inorganic mercury through erosion and surface runoff [8]. Indeed, recent studies conducted in the Cerrado biome (Central Brazil) have indicated that changes in land use in watersheds result in higher mercury concentrations in artificial [10] and natural lake sediments [11,12]. The same pattern emerged in lake sediments from watersheds affected by deforestation in the Amazon rainforest [13] and the Atlantic Forest [14]. Forest fires in Brazil are directly associated with deforestation [15] and the impacts of fires on the biogeochemical cycle of mercury have different spatial scales. Surface runoff of ash resulting from biomass burning affects aquatic ecosystems on a local scale, while atmospheric mercury emissions and its transport can influence areas located far from the fire source [16]. Therefore, the mercury dynamics in tropical regions highly threatened by anthropogenic activities need attention.

Specific physicochemical properties, such as pH, oxidation–reduction potential, dissolved oxygen, and suspended solids in solution, are important factors in mercury's availability and mobilization in freshwater ecosystems [17], since they control mercury's speciation and transport between the water column, sediment, and biological communities [18]. Sediments play a major role in the dynamics of natural aquatic systems [19] and are key to evaluating the contamination of a given water body [20]. Sediments can act as an important Hg sink and harbor micro-organisms that convert inorganic Hg into one of its organic forms, methylmercury (MeHg) [21], which is easily absorbed by the biota, therefore entering the aquatic trophic chain [22,23]. However, little is known about the influence of the interaction between geomorphology, land use, and physical–chemical water parameters on mercury concentrations in sediments. This knowledge gap is mainly due to the uneven geographical distribution of mercury research [8]. Indeed, in Brazil, studies on environmental mercury have mainly focused on the Amazon, an ecosystem of global and regional ecological relevance [24].

The Araguaia River (Central Brazil) maintains a complex mosaic of lentic and lotic ecosystems, which have a rich and diverse ichthyofauna [25], making it fundamental for the conservation of water resources and biodiversity [26]. However, the Middle Araguaia is characterized by a rapid geomorphic response to degradation by anthropogenic activities [27], so changes in land use since the 1970s have resulted in increased erosion, sandy sediment transport, and river flow [28,29]. These changes can influence local environmental characteristics and the biogeochemical cycle of mercury. A recent study indicated that the high intensity of land use in the Middle Araguaia is associated with higher water turbidity, electrical conductivity, and higher mercury concentrations in lake sediments [12]. Geology is another factor that can control the occurrence and availability of mercury in natural ecosystems. It is worth noting that the Middle Araguaia floodplain has rocks in a specific geological gradient, with plutonic igneous origin further south and sedimentary rocks to the north [30,31]. However, there still needs to be more information on the influence of geological factors on the accumulation of Hg in sediments.

Thus, this study aims to quantify mercury concentrations in the sediments of 50 natural lakes in a 750 km segment of the Middle Araguaia River (Central Brazil) to compare concentrations between lakes flowing through non-urban and urban areas of different geological origins within the Cerrado biome.

2. Materials and Methods

2.1. Study Area

The Araguaia River is the main fluvial system of Central Brazil [32]. Flowing through the Cerrado and with a small part under the Amazon rainforest, its watershed has an area close to 377,000 km^2 and a mean annual discharge of 6420 m^{3}s^{-1} [33]. This river is important to the Neotropical biodiversity [34] and has three major reaches in its 2110 km extension: upper, middle, and lower. Its lower course confluences with the Tocantins River [33], which joins the southern tributaries of the Amazon River [35].

The focus of our study is the Middle Araguaia segment. The geomorphology and flood dynamics of the Middle Araguaia result in a rich mosaic of natural lakes, characterized as abandoned channels, oxbow and meander spires, marginal dykes, and lateral accretion lakes [36]. Based on geological contact and outcrops, we identified that in the south portion of the study area, the river flows over the XambioáNeoproterozoic unit (NPx) and the Santa TerezaNeoproterozoic suite (NPgamma). In the central area, it flows over the XambioáNeoproterozoic unit (NPx), the Serra DouradaPaleoproterozoic unit (PP2sd), and the Rio dos ManguesPaleoproterozoic complex (PPgamma); while in the north section it flows over Quaternary terrains (Qag).

We surveyed the total mercury (THg) in bottom sediment from 50 lakes along 750 km of the Middle Araguaia floodplain, during the period of flood, which is when most of the lakes are navigable, to study the relationship between geological groups, land use, physicochemical variables, and THg concentrations.

We assigned each sampling point to a geological group and to one of two land uses. We labeled sampling points closer than 12 km from an urbanized area, "urban" (*n* = 16), and those farther than 12 km from an urbanized area, "non-urban" (*n* = 34). The labels for the geological groups we used were Group 1 (NPx/NPgamma), Group 2 (NPx/PP2sd/PPgamma), and Group 3 (Qag) (Figure 1).
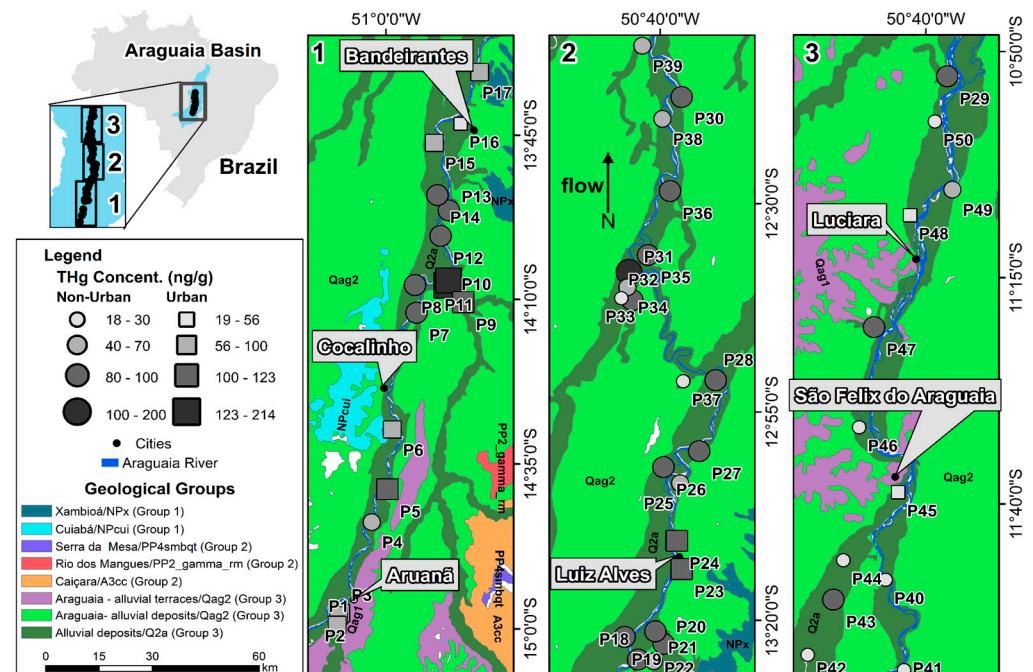

Figure 1. Location of the sampling sites, split into three different sections (**1**/south; **2**/center; **3**/north) in the Middle Araguaia River floodplain in January 2019.

2.2. Sample Collection and Mercury Determination

The collection of bottom sediment samples was conducted manually or using an Eckman dredge. All samples were stored in polyethylene bags and kept cool until sample preparation and chemical analysis. In situ measurements of pH, dissolved oxygen (DO),

temperature, oxidation–reduction potential (ORP), total dissolved solids (TDS), electrical conductivity (Ec), and turbidity levels accompanied environmental sampling at each point with a multi-parameter Horiba probe (Kyoto, Japan). Sediment samples were dried in an oven at 40 °C, followed by maceration and subjection to a sieve shaker (Bronzinox) for 10 min, to a granulometry of 600 µm, 250 µm, 120 µm, and 20 µm. After homogenization, we stored the smallest particles (20 µm) in Eppendorf® polypropylene tubes for quantification of Hg [37].

We determined THg concentrations at the Analytical and Environmental Chemistry Laboratory (LQAA) at the University of Brasilia, using atomic absorption spectrophotometry on a Lumex® Zeeman AAS RA 915+ analyzer (Lumex) with Zeeman effect correction. After weighing samples in a high precision balance, we inserted them directly into the analyzer in a quartz boat. Sample decomposition occurred in the first chamber heated up to 740 °C, and analyte atomization took place in a second heated chamber, heated up to 700 °C [38].

All glassware used for analyses was submitted to rigorous cleaning procedures that included acid washings (with HNO_3 5% for 24 h) and rinsing with ultrapure water. Analytical quality control was performed using certified reference material SS-2 (contaminated soil) and accompanied by analysis of reagent blanks, with an 88% average recovery. The coefficient of variation between replicates varied from zero to 16% and the limit of detection was 0.024 ng.

2.3. Statistical Analysis

We used multivariate analysis of variance (MANOVA) with Wilk's lambda to test the geological formation's effect on THg concentrations and related water parameters. Since we studied a route of the Araguaia River with high geological complexity and many changes in land use, we opted for the nested ANOVA model to evaluate the differences in Hg concentrations, considering the interactions of land uses (urban and non-urban), with different geological substrates. This model evaluates interactions between factor groups, without crossing factor groups. Therefore, because land uses are nested or hierarchical within the different geologies, this model is the most suitable. We assessed the significance of condition-dependent effects by considering each geological formation with its nested land use as a different condition. Having established which conditions were significant, we ran nested ANOVA to compare the averages of THg, DO, pH, temperature, ORP, TDS, electrical conductivity (Ec), and turbidity of the groups categorized by geological formation. The probability $p < 0.05$ and confidence intervals of 95% between averages showed significant differences in the tests performed. We used Tukey HSD to test the effect ($p < 0.05$) of specific groups in THg concentrations and water parameters and the Type III test to determine the effect size of each variable within each group. For this analysis, we used Group 3 non-urban for comparison. All statistical analyses were generated using Statistica 10 software (StatSoft Inc., Hamburg, Germany).

Principal Component Analysis (PCA) assessed the relationship between Hg concentrations, water physicochemical parameters, and geological formation. We employed PCA in a dataset of 300 observation values (six parameters determined at 50 sampling sites), excluding temperature and ORP due to previous results and TDS for its correlation with electrical conductivity. We performed the PCA with the prcomp function of the stats package and built a biplot with the ggbiplot function of the ggplot_pca package with R software (R Foundation, Vienna, Austria). The PCA axes were chosen based on the Kaiser–Guttman criterion, selecting only the axes with eigenvalues above one [24].

3. Results

Our results showed that land use nested in geology influenced sediment THg in lakes in the Middle Araguaia floodplain. Table 1 shows a summary of the univariate nested ANOVA for each group.

Table 1. Intercept and *p*-values from univariate analysis (nested ANOVA).

	THg [1]	DO	pH	Temp	Ec	TDS	Turb	ORP
Intercept	0.00000	0.00000	0.00000	0.00000	0.00000	0.00000	0.00000	0.00000
Geo-nested land use	0.00111	0.00502	0.00667	0.24639	0.00000	0.00000	0.08403	0.52510
Land use	0.00501	0.00406	0.00208	0.66064	0.64745	0.64717	0.30527	0.78711

[1] THg: THg in sediments; DO: dissolved oxygen; Temp: temperature; Ec: electrical conductivity; TDS: total dissolved solids; Turb: turbidity; ORP: oxidation–reduction potential.

The effect of the interaction between geology with nested land use was significant for sediment THg (Table 2).

Table 2. Mean and standard deviation values of physicochemical variables for each category.

Geology		Group 1		Group 2		Group 3	
Nested Land Use		**Urban**	**Non-Urban**	**Urban**	**Non-Urban**	**Urban**	**Non-Urban**
n	50	7	7	3	12	6	15
THg [1] (ng/g)	76.14 ± 39.03	† 119.71 ± 05.44 [a]	* 79.74 ± 14.53 [b]	* 105.40 ± 17.29 [abc]	* 81.36 ± 17.89 [bcd]	* 46.27 ± 21.37 [e]	56.05 ± 38.62 [be]
DO (mg/L)	5.57 ± 2.10	* 2.86 ± 1.81 [a]	6.00 ± 1.95 [b]	7.00 ± 0.61 [b]	6.45 ± 2.00 [b]	6.07 ± 1.92 [b]	5.43 ± 1.69 [b]
pH	6.28 ± 0.49	* 6.34 ± 0.45 [a]	* 6.31 ± 0.40 [a]	† 6.44 ± 0.20 [a]	* 6.37 ± 0.41 [a]	* 6.55 ± 0.25 [a]	6.01 ± 0.62 [b]
Turb (NTU)	6.92 ± 5.64	7.32 ± 3.92 [a]	6.58 ± 1.28 [a]	6.96 ± 1.76 [a]	10.65 ± 9.46 [ab]	3.01 ± 0.91 [ac]	5.46 ± 3.46 [ac]
Temp (°C)	30.61 ± 1.74	29.46 ± 1.09 [a]	30.32 ± 1.34 [ab]	31.58 ± 1.90 [ab]	31.38 ± 2.37 [b]	30.46 ± 0.95 [ab]	30.53 ± 1.63 [ab]
Ec (mS/cm)	0.035 ± 0.013	† 0.043 ± 0.008 [a]	* 0.036 ± 0.005 [a]	* 0.045 ± 0.007 [a]	† 0.046 ± 0.008 [a]	0.024 ± 0.008 [b]	0.026 ± 0.013 [b]
ORP	241.42 ± 54.06	244.57 ± 82.91	262.42 ± 24.79	256.00 ± 58.02	225.33 ± 54.09	221.00 ± 30.79	248.26 ± 56.38
TDS (g/L)	0.023 ± 0.008	† 0.028 ± 0.005 [a]	* 0.023 ± 0.003 [a]	* 0.029 ± 0.005 [a]	† 0.029 ± 0.005 [a]	0.015 ± 0.005 [b]	0.016 ± 0.008 [b]

* $p < 0.05$ (nested ANOVA). † $p < 0.001$ (nested ANOVA). a–e denote significant differences among columns (groups) according to Tukey's test ($p < 0.05$). [1] THg: THg in sediments; DO: dissolved oxygen; Turb: turbidity; Temp: temperature; Ec: electrical conductivity; ORP: oxidation–reduction potential; TDS: total dissolved solids.

Within Group 1, there was a statistical difference ($p = 0.02$) in sediment THg between urban and non-urban sites. THg did not vary significantly between Group 1 and Group 2, but there was a significant reduction in sediment THg in Group 3 urban sites (Table 1; Figure 2a). Figure 2 illustrates the comparison of mean values of the parameters that were under significant influence by the interaction of geology and land use and highlights statistical differences.

The MANOVA indicated that the interaction between geological groups and land use had a statistical significance ($p < 0.05$) in the physicochemical variables we analyzed, and land use was significant ($p = 0.05$) in the interaction. The univariate nested ANOVA revealed that land use had a significant impact on sediment THg; however, when we considered land use nested within the geological formation, the interaction with sediment THg became even stronger (Table 2). Type III analysis of parameters and β indicated that sediment THg was most active in Group 1 urban. The analysis removed Group 3 non-urban and used it to assess the interaction of each predictor.

Thus, regarding mercury, proximity to urbanized areas influences sediment THg levels in the Middle Araguaia floodplain; but the interaction is stronger when we consider land use nested within the geology of the area.

Land use nested in geology affected DO, pH, Ec, and TDS in lakes in the Middle Araguaia floodplain. Table 1 shows that the effect of the interaction between geology with nested land use was significant for most water variables but it was larger for Ec and TDS (Table 2). Because of the correlation between Ec and TDS, we decided to present only TDS in Figure 2.

The univariate nested ANOVA revealed that land use had a significant impact on DO ($p = 0.004$) and pH ($p = 0.002$). Additionally, when we considered land use nested within the geological formation, the interaction remained significant for DO ($p = 0.005$) and pH ($p = 0.006$) and showed an influence on Ec ($p < 0.05$) and TDS ($p < 0.05$) (Table 2).
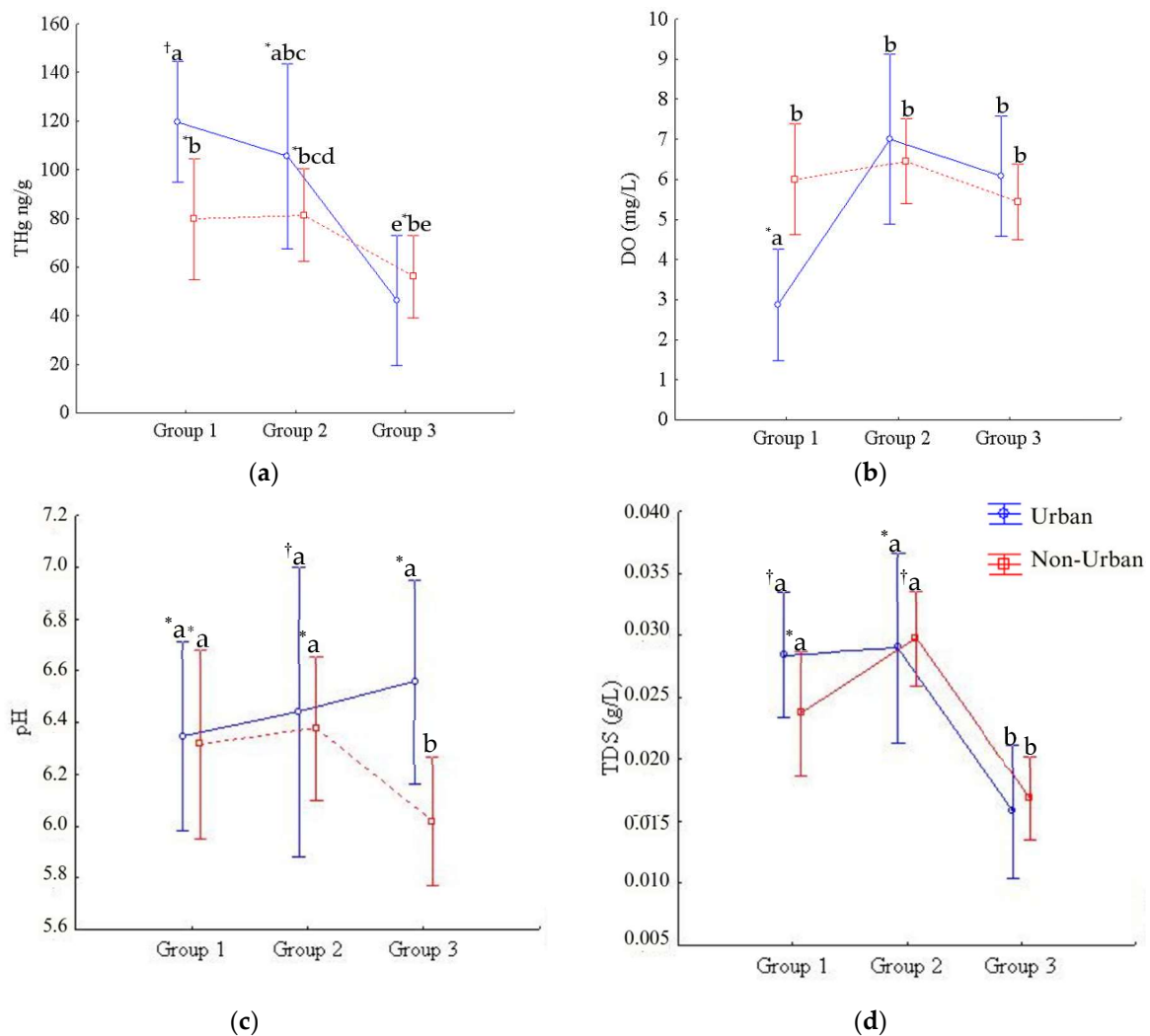
Figure 2. Differences in THg (**a**), DO (**b**), pH (**c**), and TDS (**d**), according to geological groups and land uses. Means with different letters are significantly different at † $p < 0.001$ (nested ANOVA). * $p < 0.05$ (nested ANOVA).

Tukey's test showed a significant decrease in mean DO levels in Group 1 urban (Table 1; Figure 2b) and in pH levels in Group 3 non-urban (Table 1; Figure 2c). TDS and Ec are correlated parameters; therefore, as expected, they displayed a similar statistical difference in Group 3 (Table 1; Figure 2d). Despite not being influenced by the geological groups with nested land use, we highlight that turbidity had a statistical difference between Group 2 non-urban and Group 3 ($p < 0.05$), while temperature only differed significantly between Group 1 urban and Group 2 non-urban ($p = 0.02$). However, there was no statistical difference concerning ORP (Table 1).

Type III analysis of parameters and β indicated that the most active variables in each group were as follows: Group 1 urban: THg (β = 0.57); Group 1 non-urban: Ec (β = 0.27); Group 2 urban: Ec (β = 0.34); Group 2 non-urban: Ec and TDS (β = 0.64); and Group 3 urban: pH (β = 0.36). DO showed the highest β (β = −0.42) in Group 1 urban.

Confidence intervals of 95% showed that the interaction between geology and land use was a major factor influencing the variability in sediment THg. The results allowed for the determination of which variables differed significantly among distinct geological formations with their nested land uses, and the magnitude of their influence. However, it was not possible to find a pattern. This could be due to the complexity of the study, the length of the study area, or the divergence in the number of non-urban and urban sampling sites.

The data were then subjected to a spatial multivariate statistical method to further explore spatial patterns in water physicochemical variables affected by different geological formations and proximity to urbanized areas. Principal Component Analysis (PCA) evaluated the spatial correlation and similarity of the eigenvectors with the factors scoring of the geological and land use groups. The PCA ordination of the samples is plotted in Figure 3, where it is possible to analyze how the water parameters relate to both geology (Figure 3a) and land use (Figure 3b).
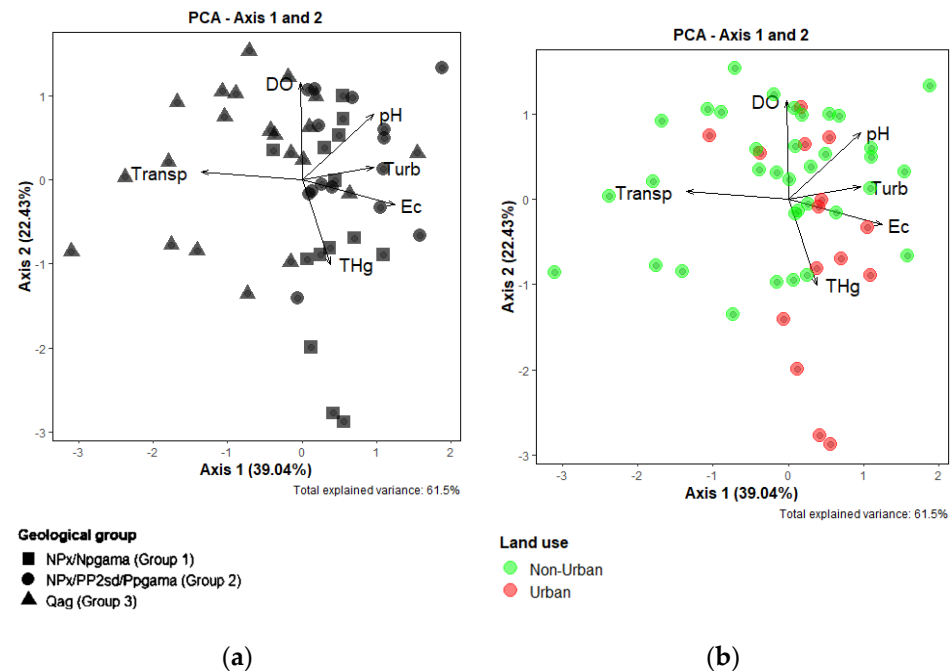

(a)   **(b)**

Figure 3. Biplots representing the ordering of variables and samples in terms of geology (**a**) and land use (**b**) according to the PCA results. THg: THg in sediments; DO: dissolved oxygen; Ec: electrical conductivity; Turb: turbidity; Transp: transparency.

The first two axes of the PCA explained 61.5% of the variation in the data (Figure 3). Axis 1 indicates the separation of the sampling units in Group 3 from those in Groups 1 and 2. There was a positive correlation of electrical conductivity, turbidity, and pH with Axis 1, mainly associated with the sampling sites in Groups 1 and 2. In contrast, water transparency, associated with Group 3, was negatively correlated with Axis 1. With Axis 2, we found a positive correlation with dissolved oxygen and pH and a negative correlation with THg concentrations in the sediment, which were predominantly associated with Group 1 sampling sites (Figure 3a). Concerning land use, there is no clear pattern of the ordering of the variables between "urban" and "non-urban" groups; however, water transparency links to the sampling sites located far from urban areas (Figure 3b).

4. Discussion

Our results indicate that sediment THg in the lakes in the Middle Araguaia River floodplain is related to the association of the geology of the area and its land use. Our statistical model revealed that sediment THg in sampling sites within Group 1 and Group 2 was significantly influenced by this interaction, which was stronger in Group 1 urban ($p < 0.001$). Despite their different geological constitution, THg concentration did not differ significantly between these groups. Group 1 (NPx/NPgamma) is made of volcanic and mafic rocks, such as biotite, muscovite, quartz, shale, granite, alkali-granite and tonalite, [30,31,39,40] while Group 2 (NPx/PP2sd/PPgamma) is constituted by volcanic, mafic and sedimentary rocks (biotite, muscovite quartz, shale, sandstone, siltstone, silt, clay, sand, and gneiss) [41–43]. Group 1 had the highest average for THg (Table 2) and there was a statistical difference between urban and non-urban within this group ($p = 0.02$). The

highest THg values were seen in urban sampling sites close to Nova Crixás (P09, P10, and P11). There was a significant reduction in THg between Groups 1/2 and Group 3 urban (Figure 2a), but there was no difference in significance between land uses in Group 3 or in Group 2.

The significant reduction in THg found in Group 3 corroborates the assumption that sedimentary rocks are not as rich in Hg as mafic and igneous rocks. Group 3 (Qag) consists of alluvial deposits [30,31] and a complex mosaic of morpho-sedimentary units formed by sediments made of laterized sandy conglomerates and other sedimentological compositions [44]. Volcanic and mafic rocks can carry a large quantity of sulfur [45] and sulfur-based compounds contribute to the metal binding capacity of freshwater wetland sediments [5]. It could also be due to the strong affinity that mercury has for organic matter, notably through binding with organic thiols [6]. The first body fossil of a microscopic metazoan was observed in rocks deposited towards the end of the Neoproterozoic period [46] and Quaternary terrains are more ancient. These results were corroborated by the Principal Component Analysis, which indicated an association between THg concentrations and geological groups constituted of volcanic and mafic rocks (NPx/NPgamma—Group 1 and NPX/PP2sd/PPgamma—Group 2) (Figure 3).

Our results partially meet the works of Tong et al. [47] and Ioele et al. [48], who concluded that urbanization has an impact on mercury content in the aquatic environment. In the Middle Araguaia floodplain, we verified this only in Group 1. This may be due to the cities surrounding the sampling points not being heavily industrialized and having small populations [49]. In addition, the discontinuity of the stable, high and flat lands along the river, as well as irregular areas, act as natural barriers to the establishment of activities such as extensive agriculture and large-scale urban infrastructure, though there are croplands in plateaus where the flat topography favors the practice of highly mechanized, intensive annual crop production [50]. The Middle Araguaia flows mainly in the lower areas of the Araguaia River Basin, which are unfavorable for large-scale land use [32,51]. Additionally, it is difficult to determine the direction of the surface runoff from agriculture or other activities.

Despite the uneven number of urban ($n = 16$) and non-urban ($n = 34$) sites, the nested analysis showed that the proximity to urbanized areas interacted significantly with the geology of the area and statistically influenced sediment mercury in the region (Table 1). However, it is noteworthy that some areas classified as non-urban had some type of anthropogenic impact, such as small-scale agriculture and livestock. Because of these findings, we highlight that the association of geological constitution and land use significantly influences the level of Hg contamination in sediments of lakes in the Middle Araguaia floodplain.

The Araguaia plain is classified as a clear water floodplain, characterized by low transport of clay sediments, low levels of organic matter, relatively high water transparency, and a pH between 5 and 8 [52]. These environmental conditions are not favorable to the accumulation of Hg in the sediments [17,53] so the presence of THg in high concentrations indicates the existence of other drivers. In the Tapajós River, for example, despite also being a clear water system, the high concentrations of Hg are associated with gold mining and large-scale deforestation in its watershed [13,54]. Although the Araguaia River and some of its tributaries have a history of artisanal gold mining, since there are several orogenic gold deposits in the area [55], we did not link it to the presence of mercury in the study area because sites that could have been influenced by this activity had average THg concentration. In this study, the interaction between geology and land use had a greater impact on THg and DO in Group 1 urban, where DO had its lowest values and sediment THg presented the highest concentrations (Figure 2). The mapping of the scores confirmed that DO and THg are inversely related in the study area (Figure 3), which indicates that the geology with its nested land use has an opposite effect on these physicochemical variables: while this interaction increases sediment THg, it decreases OD in water. However, PCA suggested a negative relation between eigenvectors THg and pH, and this differed partially

from the ANOVA results, which showed a strong effect of the interaction on pH only in Group 2 urban, where its value was not statistically different, and a negative correlation between these variables in urban sampling points. pH only varied significantly in Group 3 non-urban surroundings, where it showed the lowest values, but THg concentrations were also low in this area. pH interferes in the production of dimethylmercury and monomethylmercury, but the total amount of mercury methylated remains approximately the same [56]; therefore, it is acceptable that pH does not interfere with the amount of THg.

In our study, we found that the interaction between geological constitution and land use in the Middle Araguaia River floodplain influences TDS and conductivity significantly, especially in Group 1 urban and Group 2 non-urban. They varied comparably with THg, with the lowest values in Group 3 areas. TDS concentration describes the presence of inorganic salts and small amounts of organic matter in the water while conductivity is the measure of water's capacity to conduct electrical current and these parameters correlate. The sources of material in TDS and conductivity can come from nature, i.e., geological conditions and seawater, and from human activities, i.e., domestic and industrial waste and agriculture [57]. Since Hg, TDS, and electrical conductivity have similar sources, it is reasonable that they display comparable behavior.

Concerning turbidity, initially, the ANOVA indicated that the interaction between geology and land use did not have a significant influence on lakes in the Middle Araguaia floodplain (Table 1). However, when we analyzed the effect on each group, there was a statistical difference in Group 2 non-urban. The turbidity measured in nephelometric turbidity units (NTU) is often used as a rough index of the fine suspended sediment content of the water [58], so we believe that this portion of the study area must present a higher rate of erosion, which knowingly contributes enormous amounts of fine suspended sediment and consequent turbidity to river and lakes. We found no effect of the interaction between geology and land use over temperature or ORP in the lakes in the Middle Araguaia floodplain.

5. Conclusions

This study focused on the total mercury concentrations in the bottom sediments of lakes in the Middle Araguaia River, Brazil. Spatial variation in THg in the samples from each of the 50 stations provided strong indications that the geological constitution associated with land use explains its distribution in the area. Sampling sites in regions of mafic rocks and close to urbanized areas had the highest values for THg. In the Middle Araguaia floodplain, both the geological constitution and proximity to urbanized areas influence sediment THg, but the effect is greater when their interaction is considered.

We found that this interaction also influences water physicochemical variables. pH values were significantly lower in Group 3 non-urban areas, while DO showed a significant difference in Group 2 urban areas. Turbidity varied significantly among the assigned groups, as did TDS and conductivity in water suffer influence from this interaction. However, we could not establish a relationship between geological formations with their nested land use and ORP or temperature.

Our study provides new data on the presence of Hg in a tropical region that is part of an extremely important biome, the Cerrado. The gathered data may be extremely useful for comparison with similar areas in the world and can contribute to understanding the ecological risks of anthropic influence in the Cerrado, as well as support decision-making policies aimed at public health and Hg pollution control in the Tocantins–Araguaia basin.

Author Contributions: Conceptualization, L.M., J.V.E.B., L.C.G.V., C.J.S.P., J.R.d.S., W.R.B. and J.G.D.; methodology, L.M., L.C.G.V., J.R.d.S., W.R.B. and J.V.E.B.; software, L.M., L.C.M., Y.O.S.R. and J.V.E.B.; validation, J.G.D., J.F.P., J.R.d.S., W.R.B. and J.P.R.d.S.; formal analysis, L.M., J.V.E.B., J.R.d.S., W.R.B., J.F.P., L.C.M., Y.O.S.R. and J.P.R.d.S.; investigation, L.M. and J.V.E.B.; resources, J.G.D., J.V.E.B., L.C.G.V., J.R.d.S., W.R.B. and J.F.P.; data curation, J.V.E.B. and L.M.; writing—original draft preparation, L.M., L.C.M., Y.O.S.R., J.F.P. and J.P.R.d.S.; writing—review and editing, L.M., J.V.E.B. and J.G.D.; visualization, J.V.E.B. and L.M.; supervision, J.G.D., C.J.S.P., J.R.d.S. and W.R.B.; project

References

1. Jardim, W.F.; Bisinoti, M.C.; Fadini, P.S.; Silva, G.S. Mercury redox chemistry in the Negro Riverbasin, Amazon: The role of or ganic matter and solar light. *Aquat. Geochem.* **2010**, *16*, 267–278. [CrossRef]
2. Pirrone, N.; Cinnirella, S.; Feng, X.; Finkelman, R.B.; Friedli, H.R.; Leaner, J.; Mason, R.; Mukherjee, A.B.; Stracher, G.B.; Streets, D.G.; et al. Global mercury emissions to the atmosphere from anthropogenic and natural sources. *Atmos. Chem. Phys.* **2010**, *10*, 5951–5964. [CrossRef]
3. Driscoll, C.T.; Mason, R.P.; Chan, H.M.; Jacob, D.J.; Pirrone, N. Mercury as a global pollutant—Sources, pathways, and effects. *Environ. Sci. Technol.* **2013**, *47*, 4967–4983. [CrossRef] [PubMed]
4. Lintern, A.; Schneider, L.; Beck, K.; Mariani, M.; Fletcher, M.-S.; Gell, P.; Haberle, S. Background concentrations of mercury in Australian freshwater sediments: The effect of catchment characteristics on mercury deposition. *Elem. Sci. Anthr.* **2020**, *8*, 19. [CrossRef]
5. King, J.K.; Harmon, S.M.; Fu, T.T.; Gladden, J.B. Mercuryremoval, methylmercury formation, and sulfate-reducing bacteria profiles in wetland mesocosms. *Chemosphere* **2002**, *46*, 859–870. [CrossRef]
6. Hazen, R.M.; Golden, J.; Downs, R.T.; Hystad, G.; Grew, E.S.; Azzolini, D.; Sverjensky, D. Mercury (Hg) mineralevolution: A mineralogical record of supercontinent assembly, changing ocean geochemistry, and the emerging terrestrial biosphere. *Am. Mineral.* **2012**, *97*, 1013–1042. [CrossRef]
7. Outridge, P.M.; Mason, R.P.; Wang, F.; Guerrero, S.; Heimburger-Boavida, L.E. Updated Global and Oceanic Mercury Budgets for the United Nations Global Mercury Assessment 2018. *Environ. Sci. Technol.* **2018**, *52*, 11466–11477. [CrossRef]
8. Fisher, J.A.; Schneider, L.; Fostier, A.H.; Guerrero, S.; Guimarães, J.R.D.; Labuschagne, C.; Leaner, J.L.; Martin, L.G.; Mason, R.P.; Somerset, V.; et al. A synthesis of mercury research in the Southern Hemisphere, part 2: Anthropogenic perturbations. *Ambio* **2023**, *52*, 918–937. [CrossRef]
9. MapBiomas. Relatório Anual do Desmatamento do Brasil—2022. 2023. Available online: https://alerta.mapbiomas.org/relatorio (accessed on 17 July 2023).
10. Portela, J.F.; Souza, J.P.R.; Tonhá, S.; Bernbardi, J.V.E.; Garnier, J.; Souza, J.R. Evaluation of Total Mercury in Sediments of the Descoberto River Environmental Protection Area—Brazil. *Int. J. Environ. Res. Public Health* **2020**, *17*, 154. [CrossRef]
11. Dórea, J.G.; Monteiro, L.C.; Bernardi, J.V.E.; Fernandes, I.O.; Oliveira, S.F.B.; Souza, J.P.R.; Rosrigues, Y.O.S.; Vieira, L.C.G.; Souza, J.R. Landuse impact on mercury in sediments and macrophytes from a natural lake in the Brazilian savanna. *Environ. Pollut.* **2023**, *337*, 15. [CrossRef]
12. Monteiro, L.C.; Viera, L.C.G.; Bernardi, J.V.E.; Moraes, L.C.; Rodrigues, Y.O.S.; Souza, J.P.R.; Souza, J.R.; Bastos, W.R.; Passos, C.J.S.; Dorea, J.G. Ecological risk of mercury in bottom sediments and spatial correlation with landuse in Neotropical savanna floodplain lakes, Araguaia River, Central Brazil. *Environ. Res.* **2023**, *238*, 117231. [CrossRef] [PubMed]
13. Oestreicher, J.S.; Lucotte, M.; Moingt, M.; Bélanger, E.; Rozon, C.; Davidson, R.; Mertens, F.; Romaña, C.A. Environmental and anthropogenic factors influencing mercury dynamics during the past century in floodplain lakes of the Tapajós River, Brazilian Amazon. *Arch. Environ. Contam. Toxicol.* **2017**, *72*, 11–30. [CrossRef] [PubMed]
14. Lima, C.A.I.; Almeida, M.G.; Pestana, I.A.; Bastos, W.R.; Recktenvald, C.N.; Souza, C.M.M.; Pedrosa, P. Impact of Land Use on the Mobility of Hg Species in Different Compartments of a Tropical Watershed in Brazil. *Arch. Environ. Contam. Toxicol.* **2017**, *73*, 578–592. [CrossRef] [PubMed]
15. Silva, C.A.; Santilli, G.; Sano, E.E.; Laneve, G. Fire Occurrences and Greenhouse Gas Emissions from Deforestation in the Brazilian Amazon. *Remote Sens.* **2021**, *13*, 376. [CrossRef]
16. López, A.F.; Barrón, E.G.H.; Bugallo, P.M.B. Contribution to understanding the influence of fires on the mercury cycle: Systematic review, dynamic modeling and application to sustainable hypothetical scenarios. *Environ. Monit. Assess.* **2022**, *194*, 707. [CrossRef]
17. Vieira, M.; Bernardi, J.V.E.; Dorea, J.G.; Rocha, B.C.P.; Ribeiro, R.; Zara, L.F. Distribution and availability of Mercury and methylmercury indifferent waters from the Rio Madeira Basin, Amazon. *Environ. Pollut.* **2018**, *235*, 771–779. [CrossRef]
18. Gabriel, M.C.; Williamson, D.G. Principal biogeochemical factors affecting the speciation and transport of mercury through the terrestrial environment. *Environ. Geochem. Health* **2004**, *26*, 421–434. [CrossRef] [PubMed]

19. Pelcová, P.; Margetínová, J.; Vaculovic, T.; Komarek, J.; Kuban, V. Adsorption of mercury species on riversediments—Effects of selected abiotic parameters. *Cent. Eur. J. Chem.* **2010**, *8*, 116–125. [CrossRef]

20. Cardoso-Silva, S.; Ferreira, P.A.L.; Moschini-Carlos, V.; Figueira, R.C.L.; Pompêo, M. Temporal and spatial accumulation ofheavy metals in the sediments at Paiva Castro Reservoir (São Paulo, Brazil). *Environ. Earth Sci.* **2016**, *75*, 9. [CrossRef]

21. Zhang, L.; Wu, S.; Zhao, L.; Lu, X.; Pierce, E.M.; Gu, B. Mercury sorption and desorption on organo-mineral particulates as a source for microbial methylation. *Environ. Sci. Technol.* **2019**, *53*, 2426–2433. [CrossRef]

22. Gustin, M.S.; Evers, D.C.; Bank, M.S.; Hammerschimidt, C.R.; Pierce, A.; Basu, N.; Blum, J.; Bustamante, P.; Chen, C.; Driscoll, C.T.; et al. Importance of integration and implementation of emerging and future mercury research in to the Minamata Convention. *Environ. Sci. Technol.* **2016**, *50*, 2767–2770. [CrossRef] [PubMed]

23. Lavoie, R.A.; Jardine, T.D.; Chumchal, M.M.; Kidd, K.A.; Campbell, L.M. Biomagnification of Mercury in Aquatic Food Webs: A Worldwide Meta-Analysis. *Environ. Sci. Technol.* **2013**, *47*, 13385–13394. [CrossRef] [PubMed]

24. Pinto, L.C.M.; Dorea, J.G.; Bernardi, J.V.E.; Gomes, L.F. Mapping the Evolution of Mercury (Hg) Research in the Amazon (1991–2017): A Scientometric Analysis. *Int. J. Environ. Res. Public Health* **2019**, *16*, 1111. [CrossRef] [PubMed]

25. Tejerina-Garro, F.L.; Fortin, R.; Rodríguez, M.A. Caracterização da ictiofauna e das interações peixe-ambiente no médio Araguaia, baciaAmazônica. *Estudos* **2002**, *29*, 87–101.

26. Latrubesse, E.M.; Arima, E.; Ferreira, M.E.; Nogueira, S.H.; Wittmann, F.; Dias, M.S.; Dagosta, F.C.P.; Bayer, M. Fostering water resource governance and conservation in the Brazilian Cerrado biome. *Conserv. Sci. Pract.* **2019**, *1*, e77. [CrossRef]

27. Suizu, T.M.; Latrubesse, E.M.; Stevaux, J.C.; Bayer, M. Resposta da morfologia do médio-curso superior do Rio Araguaia às mudanças no regime hidrossedimentar no período 2001–2018. *Rev. Bras. Geomorfol.* **2022**, *23*, 1420–1434. [CrossRef]

28. Latrubesse, E.M.; Amsler, M.L.; de Morais, R.P.; Aquino, S. The geomorphologic response of a large pristine alluvial river to tremendous deforestation in the South American tropics: The case of the Araguaia River. *Geomorphology* **2009**, *113*, 239–252. [CrossRef]

29. Coe, M.T.; Latrubesse, E.M.; Ferreira, M.E.; Amsler, M.L. The effects of deforestation and climate variability on the streamflow of the Araguaia River, Brazil. *Biogeochemistry* **2011**, *105*, 119–131. [CrossRef]

30. Bizzi, L.A.; Schobbenhaus, C.; Vidotti, R.M.; Gonçalves, J.H. *Geologia, Tectônica e Recursos Minerais do Brasil: Texto, Mapas & SIG*; CPRM—Serviço Geológico do Brasil: Brasília, Brazil, 2003.

31. Ferreira, R.V.; Shinzato, E.; Dantas, M.E.; Teixeira, W.G. Origem das paisagens do estado do Pará. In *Geodiversidade do Estado do Pará*; Teixeira, S.G., João, X.J., Eds.; CPRM—Serviço Geológico do Brasil: Brasília, Brazil, 2011; pp. 23–52.

32. Valente, C.R.; Latrubesse, E.M.; Ferreira, L.G. Relationships among vegetation, geomorphology and hydrology in the Bananal Island tropical wetlands, Araguaia River basin, Central Brazil. *J. S. Am. Earth Sci.* **2013**, *46*, 150–160. [CrossRef]

33. Latrubesse, E.M.; Stevaux, J.C. Geomorphology and environmental aspects of the Araguaia fluvial basin, Brazil. *Z. Geomorphol.* **2002**, *129*, 109–127.

34. Jarduli, L.R.; Claro-García, A.; Shibatta, O.A. Ichthyofauna of the rio Araguaia basin, states of Mato Grosso and Goiás, Brazil. *Check List* **2014**, *10*, 483–515. [CrossRef]

35. Costa, M.H.; Botta, A.; Cardille, J.A. Effects of large-scale changes in land cover on the discharge of the Tocantins River, Southeastern Amazonia. *J. Hydrol.* **2003**, *283*, 206–217. [CrossRef]

36. Morais, R.P.; Oliveira, L.G.; Latrubesse, E.M.; Pinheiro, R.C.D. Morfometria de sistemas lacustres da planície aluvial do médio rio Araguaia. *Acta Sci.* **2005**, *27*, 203–213. [CrossRef]

37. Rodrigues, Y.O.S.; Dorea, J.G.; Landim, P.M.B.; Bernardi, J.V.E.; Monteiro, L.C.; Souza, J.P.R.; Pinto, L.C.M.; Fernandes, I.O.; Souza, J.V.V.; Sousa, A.R. Mercury spatiality and mobilization in roadside soils adjacent to a savannah ecological reserve. *Environ. Res.* **2022**, *205*, 112513. [CrossRef] [PubMed]

38. Sholupov, S.; Pogarev, S.; Ryzhov, V.; Mashyanov, N.; Stroganov, A. Zeeman atomic absorption spectrometer RA-915+ for direct determination of mercury in air and complex matrix samples. *Fuel Process. Technol.* **2004**, *85*, 473–485. [CrossRef]

39. Hasui, Y.; Abreu, F.D.A.M.; Silva, J.M.R. Estratigrafia da faixa de dobramentos Paraguai-Araguaia no centro-norte do Brasil. *Bol. IG* **1977**, *8*. [CrossRef]

40. Moura, C.A.V.; Pinheiro, B.L.S.; Nogueira, A.C.R.; Gorayeb, P.S.S.; Galarza, M.A. Sedimentary provenance and palaeoenvironment of the Baixo Araguaia Supergroup: Constraints on the palaeogeographical evolution of the Araguaia Belt and assembly of West Gondwana. *Geol. Soc. Spec. Publ.* **2008**, *294*, 173–196. [CrossRef]

41. Araujo, S.M.; Fawcett, J.J.; Scott, S.D. Metamorphism of hydrothermally altered rocks in a volcanogenic massive sulfide deposit: The Palmeirópolis, Brazil. *Rev. Bras. Geociências* **1995**, *25*, 173–184. [CrossRef]

42. Corrêa, L.W.C.; Macambira, M.J.B. Evolução da região de Santana do Araguaia (PA) com base na geologia e geocronologia Pb-Pb em zircão de granitoides. *Geol. USP-Ser. Cient.* **2014**, *14*, 45–66. [CrossRef]

43. LeaoNeto, R.; Oliviatti, O. *Projeto Palmeirópolis-Etapa Preliminar: Goiania*; CPRM—Companhia de Pesquisa e Recursos Minerais: Brasília, Brazil, 1983.

44. Morais, R.P.; Aquino, S.; Latrubesse, E.M. Controles hidrogeomorfológicos nas unidades vegetacionais da planície aluvial do rio Araguaia, Brasil. *Acta Sci.-Biol. Sci.* **2008**, *30*, 411–421. [CrossRef]

45. Peng, G.; Luhr, J.F.; McGee, J.J. Factors controlling sulfur concentrations in volcanic apatite. *Am. Mineral.* **1997**, *82*, 1210–1224. [CrossRef]

46. Khan, I.; Zhong, N.; Luo, Q.; Ai, J.; Yao, L.; Luo, P. Maceral composition and origin of organic matter input in Neoproterozoic—Lower Cambrian organic-rich shales of Salt Range Formation, upper Indus Basin, Pakistan. *Int. J. Coal Geol.* **2020**, *217*, 103319. [CrossRef]

47. Tong, Y.; Zhang, W.; Hu, D.; Ou, L.; Hu, X.; Yang, T.; Wei, W.; Ju, L.; Wang, X. Behavior of mercury in an urban river and its accumulation in aquatic plants. *Environ. Earth Sci.* **2013**, *68*, 1089–1097. [CrossRef]

48. Ioele, G.; Luca, M.; Grande, F.; Durante, G.; Trozzo, R.; Crupi, C.; Ragno, G. Assessment of Surface Water Quality Using Multivariate Analysis: Case Study of the Crati River, Italy. *Water* **2020**, *12*, 2214. [CrossRef]

49. Estimativas de População Enviadas ao TCU. Available online: https://www.ibge.gov.br/estatisticas/sociais/populacao/9103-estimativas-de-populacao.html (accessed on 10 December 2021).

50. Martins, P.R.; Sano, E.E.; Martins, E.S.; Vieira, L.C.G.; Salemi, L.F.; Vasconcelos, V.; Couto Junior, A.F. Terrain units, land use and land cover, and gross primary productivity of the largest fluvial basin in the Brazilian Amazonia/Cerrado ecotone: The Araguaia River basin. *Appl. Geogr.* **2021**, *127*, 102379. [CrossRef]

51. Valente, C.R.; Latrubesse, E.M. Fluvial archive of peculiar avulsive fluvial patterns in the largest Quaternary intracratonic basin of tropical South America: The Bananal Basin, Central-Brazil. *Palaeogeogr. Palaeoclimatol. Palaeoecol.* **2012**, *356–357*, 62–74. [CrossRef]

52. Irion, G.; Nunes, G.M.; da Cunha, C.N.; Arruda, E.C.; Tambelini, M.S.; Dias, A.P.; Morais, J.O.; Junk, W.J. Araguaia River Floodplain: Size, Age, and Mineral Composition of a Large Tropical Savanna Wetland. *Wetlands* **2016**, *36*, 945–956. [CrossRef]

53. Lacerda, L.D.; Paula, F.C.F.; Ovalle, A.R.C.; Pfeiffer, W.C.; Malm, O. Trace metals in fluvial sediments of the Madeira River watershed, Amazon, Brazil. *Sci. Total Environ.* **1990**, *97–98*, 525–530. [CrossRef]

54. Berzas Nevado, J.J.; Martín-Doimeadios, R.C.R.; Bernardo, F.J.G.; Moreno, M.J.; Herculano, A.M.; Nascimento, J.L.M.; Crespo-López, M.E. Mercury in the Tapajós River basin, Brazilian Amazon: A review. *Environ. Int.* **2010**, *36*, 593–608. [CrossRef]

55. Campos, M.L.; Toledo, C.L.B.; Silva, A.M.; Ducart, D.F.; dos Santos, B.A.; Campos, M.P.; Borges, C.C.A. The hydrothermal footprint of the Crixás deposit: New vectors for orogenic gold exploration in central Brazil. *Ore Geol. Rev.* **2022**, *146*, 104925. [CrossRef]

56. Winfrey, R.; Rudd, W.M. Formation of methylmercury in low pH lakes. *Environ. Toxicol. Chem.* **1990**, *9*, 853–869. [CrossRef]

57. Rusydi, A.F. Correlation between conductivity and total dissolved solid in various type of water: A review. *IOP Conf. Ser. Earth Environ. Sci.* **2018**, *118*, 012019. [CrossRef]

58. Davies-Colley, R.J.; Smith, D.G. Turbidity, suspended sediment, and waterclarity: A review. *J. Am. Water Resour. Assoc.* **2001**, *37*, 1085–1101. [CrossRef]